BC170-99

Observation of an enhanced ballistic phonon fraction for surface events in a cryogenic silicon detector

R.M.Clarke, P.L. Brink, P. Colling, M.B. Crisler, A.K. Davies, S. Eichblatt, R.J. Gaitskell[1], J. Helmig[1], S.W. Nam, T. Saab, B.A. Young[2],B. Cabrera

Physics Department, Stanford University, Stanford, CA 94305, USA

[1] *Center for Particle Astrophysics, University of California, Berkeley, CA 94720, USA*

[2] *Santa Clara University, Department of Physics, Santa Clara, CA 95053*

Abstract

We present evidence of an enhanced ballistic phonon component resulting from surface events in a 100 g silicon cryogenic dark matter detector. Surface events, calibrated using a ^{14}C electron source, were found to have faster rise times ($\sim 5\,\mu s$) than bulk gamma and neutron events ($\sim 7\mu s$). Using this effect we were able to discriminate a surface electron background at the 97% level above 25 keV recoil energy. The phonon rise time for bulk gamma events was dependent on the applied voltage, confirming that phonons produced from electron-hole emission are ballistic.

Key words: cryogenic detectors, dark matter, phonon-mediated, athermal phonon, ballistic phonon, calorimeters, quasiparticle-trap-assisted, transition-edge sensor.
29.40.Vj, 63.20.-e

Typeset using REVTEX

By combining low temperature phonon measurements with conventional ionization measurement [1,2], large mass dark matter detectors have been developed with a high degree of background rejection capability. The decreased ionization yield due to the nuclear recoil quenching factor [3] has enabled these detectors to discriminate between bulk gamma and nuclear recoil events at better than the 99% level [4]. Surface events, although they are not subject to nuclear quenching, produce fewer electron-hole (e-h) pairs than a photon of the equivalent recoil energy (E_r) which interacts deep within the crystal. The presence of this 'dead layer' [5] severely limits the ability of these detectors to discriminate between bulk nuclear recoils and a soft beta ($E_r \lesssim 100\,\mathrm{keV}$) background component. Our experiments utilize a new generation cryogenic dark matter detector utilizing a quasiparticle-trap-assisted electrothermal feedback transition-edge-sensor (QET) [6]. This type of phonon sensor is intrinsically fast ($t_{rise} \simeq 5\,\mu\mathrm{s}$, $t_{fall} \simeq 100\,\mu\mathrm{s}$) and has the ability image the event location in a 3 inch diameter crystal using phonon propagation delay (Fig.1a) [7].

The phonons that reach the sensor can be generated in a variety of ways. Particle interactions in silicon create primarily high frequency phonons that quickly undergo anharmonic decay ($\Gamma_D \propto \nu^{-5}$), and diffuse due to isotopic scattering ($\Gamma_I \propto \nu^{-4}$). The combination of the two scattering mechanisms create a phenomenon known as quasi-diffusive transport [8]. Over microsecond timescales phonons approach an average frequency of $\approx$1 THz [9], and take longer than the ballistic time ($t \sim 3t_b$) to reach the surface of the detector. Phonons generated by e-h pairs drifting through the crystal due to the electric field of the ionization bias [10] are predicted to of be lower frequency [11] and thus travel ballistically. Previous estimates of the fraction of phonon energy propagating ballistically for electron recoils in silicon detectors [12] were small ($\sim$0.9%). Measurements of alpha induced phonons, however, indicated large ballistic components [13] (30%). Here we show that the discrepancy in these two estimates can be explained by the downconversion of phonons at the surface by thin film metalic layers.

The detector consists of thin film metalic layers fabricated on a 10 mm thick 76 mm diameter crystal of high purity ($\rho > 8\,\mathrm{k}\Omega$-cm) silicon. The phonon side is covered (90%) with

150 nm Al and a 25 nm W grid (10% area coverage, 20 μm spacing) around the outer perimeter. The gap between Al elements never exceeds 100 μm to ensure uniformity of the electric field. Many 2 μm lines of W (<1 mm^2 total area) are interspersed throughout the phonon side to form the transition edge sensor (TES). Four separate channels are instrumented (see inset Fig.1a) to allow the reconstruction of event location through phonon delay timing. The ionization side consists of a 20% area coverage grid (spacing 25 μm) of 5 nm/25 nm Ti/Au. Details of sensor geometry and design can be found in ref. [14].

When athermal phonons ($E_{ph} > 2\Delta_{Al}$) from a particle event reach the surface of the detector, they scatter in the large area ($\sim$1 mm) Al fins and generate quasiparticles. These quasiparticles then diffuse into 444 tungsten TES elements, connected in parallel, that are voltage biased within their superconducting transition (T_c=65 mK). The resulting current pulse is read out by a high-bandwidth (1 MHz) SQUID array [15]. All processes involved are intrinsically faster than the phonon transit times with the exception of the quasiparticle lifetime for trapping, estimated to be $\approx 3\,\mu s$.

A ^{14}C electron source was mounted on the ionization readout side of the detector 10 mm from the surface. Four collimator holes, $\sim$25 mm apart, produced a combined rate of $\sim$100 Hz and spot sizes on the surface $\sim$3 mm in diameter. An ^{241}Am source was mounted on the opposite side (phonon side, see inset Fig.1b) to provide 60 keV photons. The detector was cooled to 30 mK using an Oxford Instruments 75 μW dilution refrigerator. Phonon and ionization pulses were digitized at 10 MHz with a total record of 1 ms.

By comparing the delay between the 4 phonon sensors (CD-AB) vs. (BC-AD), the 4 collimated spots from the electron source were easily separated from the uniform backgound (see Fig.1a)). Figure 1b shows the distribution of electrons at 5 μs rise time with a recoil spectrum consistent with the allowed beta spectrum of ^{14}C. The 60 keV photons showed a rise time distribution peaked at 7.5 μs with a 1σ width of 0.75 μs. The tail in the 60 keV photon distribution extending to low rise time and low charge collection ($y \equiv n_{eh}/E_r$) and can be attributed to photons interacting close to the (charge side) surface. This feature enabled us to estimate the characteristic length scale of $\sim$300 μm for the rise time enhancement depth. To explain this effect we construct a simple model where initial phonons interact in the metalic surface layer (25 nm Au grid) and heat it locally to above 1K. The metal then reradiates a Plankian distribution of phonons [16] which travel ballistically across the detector. This model gives a distance scale of $\sim 100\,\mu$m where the local energy density is high enough to heat the gold layer to 1K, relatively consistent with our measured value.

In another experiment we measured the nuclear recoil response of the detector using a ^{252}Cf neutron source placed 0.5 m from the cryostat. Figure 2a shows the ability of the detector to separate neutron, gamma and beta events at 50-70 keV (chosen to include the 60 keV gammas). Electrons and neutrons both appear with low y but are separated using the phonon rise time. To separate the (traditional) y discrimination from rise time we performed a cut in y (shown as the vertical dotted lines in Figure 2a. We then define in the usual way [17] a quality factor,

$$Q = \frac{\beta(1-\beta)}{(\alpha-\beta)^2} \tag{1}$$

where β is the fraction of background events (electrons) and α is the fraction of signal events (neutrons) that survive. The quantity Q gives the fractional reduction in the signal upper limit as $\sqrt{Q/MT}$ after performing statistical background subtraction (M≡mass,T≡time). The variation of Q with rise time (cut position) is shown in Figure 2b(inset)) for 50-70 keV. This minimum is plotted as a function of energy in Figure 2b. The rise in Q at low energy is caused by detector noise.

The ionization bias voltage was varied from 0 to 3 volts during another experiment. This range caused the fraction of phonons, shed by electron hole pairs, to increase from zero to 44% (a correction for charge collection efficiency was applied) and the rise time of the 60 keV signal to decrease from $\sim 8\,\mu$s to $\sim 6.5\mu$s (Fig.3). With a simple model of our detector response we were able to simulate this effect using two populations of phonons. The first population arrives with a 8.6 μs characteristic fall time (30% absorption at the phonon detector, ballistic velocity) and the other with a 25.8 μs fall time (consistent with v$\sim \frac{v_b}{3}$). The detector was modelled using two single pole filters of 2.5 μs for the quasiparticle relaxation time and 10 μs for the ETF response time [14].

In these series of experiments we have demonstrated the ability to use phonon rise time to discriminate between bulk nuclear and surface electron events. The effect is likely due to the downconversion of high frequency phonons that interact with metalic layers at the surface of the detector. The variation of rise time with applied voltage points strongly to the generation of ballistic phonons by drifting electron-hole pairs, which may prove useful in future phonon-based discrimination schemes.

This work was generously supported by the Department of Energy under contracts DE-FG03-90ER40569, DE-FG03-91ER40618 and DE-AC03-76SF00098, by the Center for Particle Astrophysics (an NSF Science and Technology Center operated by the University of California, Berkeley) under Cooperative Agreement No. AST-91-20005. We gratefully acknowledge the skillful and dedicated efforts of the technical staffs at FermiLab, LBNL, Stanford University, UC Berkeley, and UC Santa Barbara.

REFERENCES

[1] N.E. Booth *et al.*, *Ann. Rev. Nucl. Part. Sci.* **46**, 471 (1996). **More Refs**

[2] D. Yvon *et al.*, *J. Low Temp. Phys.* **93**, 405 (1993).

[3] J. Lindhard *et al.*, *Nat. Fys. Medd. Dan. Selsk* **33**, 10 (1963). B.L. Dougherty, *et al.*, *Phys. Rev.* A **45**, 2104 (1992).

[4] T. Shutt *et al.*, *Phys. Rev. Lett.* **69**, 3531 (1992).

[5] T. Shutt *et al.*, Proc. Seventh Int. Low Temp. Det. LTD-7, 224 (1997).

[6] K.D. Irwin *et al.*, *Appl. Phys. Lett.* **66**, 1998 (1995). S.W. Nam *et al.*, Proc. Sixth Int. Low Temp. Det. LTD-6, 187 (1996).

[7] P.L. Brink *et al.*, *Czech. J. Phys.* **46**, 2887 (1996). B. Cabrera *et al Proceedings of idm96*

[8] Y.B. Levinson, *Phonon Propagation with Frequency Downconversion*, in Nonequilibrium Phonons in Nonmetallic Crystals, eds W. Eisenmenger and A.A. Kaplyanskii, p. 91. (Elsivier, 1986)

[9] S. Tamura *et al.*, *Phys. Rev.* B **56**, 13630 (1997).

[10] B.Neganov *et al.*, Otkrytia: Izobreteniya **146**, 215 (1985). P.L.Luke, *J. Appl. Phys.* **64**, 6858 (1988).

[11] B. Cabrera *et al.*, *J. Low Temp. Phys.*, proceedings of LTD-5, 1993,Vol. 93, p.365.

[12] A.T. Lee *et al.*, *Phys. Rev.* B **54**, 3244 (1996).

[13] B.A. Young *et al.*, *Phys. Rev. Lett.* **64**, 2795 (1990).

[14] R.M. Clarke *et al.*, Proc. Seventh Int. Low Temp. Det. LTD-7, 229 (1997). R.M. Clarke *et al.*, (unpublished).

[15] R.P.Welty, J.P.Martinis, *IEEE Trans. Magn.* **27**, 2924 (1991). *IEEE Trans. Appl. Supercon.* **3**, 2605 (1993).

[16] For many references see Imaging Phonons, J.P. Wolfe

[17] P.F. Smith and J.D. Lewin, *Astroparticle Physics* **6**, 87 (1996). R.J. Gaitskell, *et al.*, *Nucl. Phys. B*, Proc. Suppl., Santa Monica, 1996, p. 279.

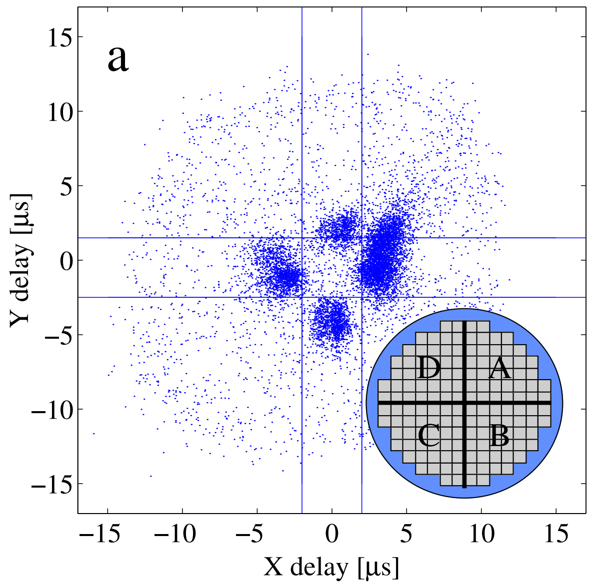

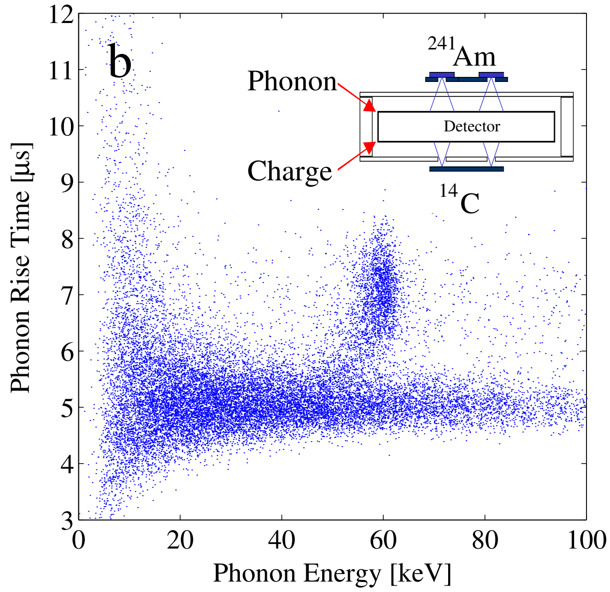

FIG. 1. a) Phonon delay in X (CD-AB) vs. delay in Y (BC-AD) for 60 keV. Inset: The four phonon sensor geometry. The four collimated distributions from the ^{14}C source are clearly visible above the uniform background (r $\sim 15\,\mu$s). The ^{241}Am source forms two spots (obscured by the electrons) on the x-axis. b) Phonon rise time vs. phonon energy for events near zero X or Y delay (see a). Inset: Detector and source geometry.

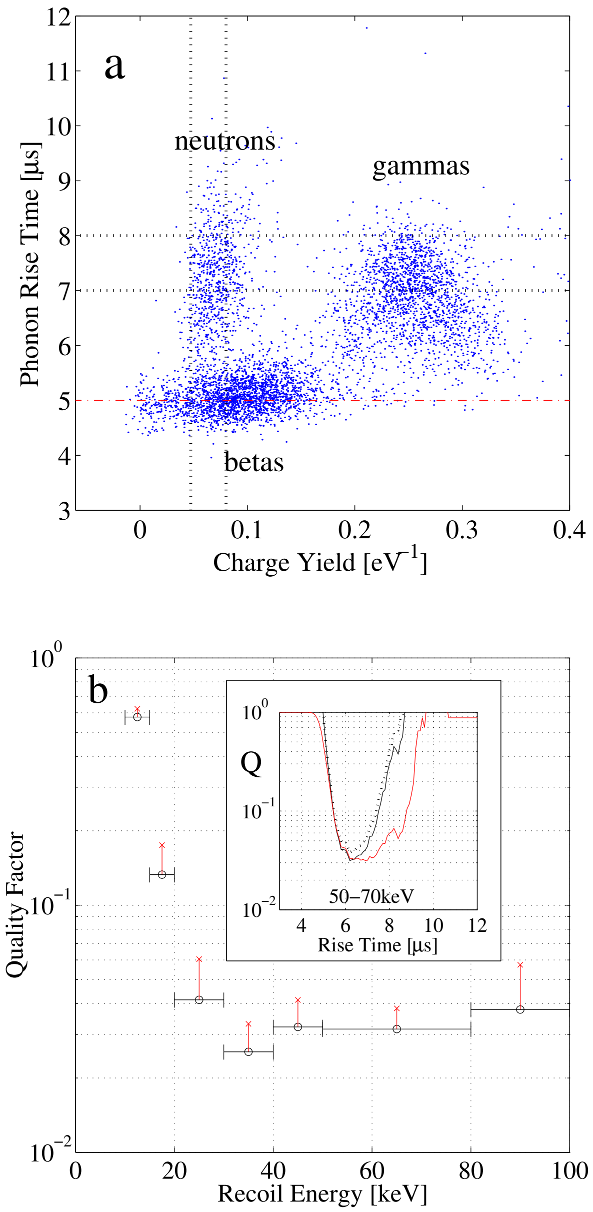

FIG. 2. a) Phonon rise time (t_r) vs. charge yield (y) for 50-70 keV recoil energy. Electrons form a distribution on the lower left (low y and fast t_r), Neutrons upper left (low y and slow t_r), and gammas (large y) upper right. Dotted lines are used to define a quality factor (Q) for pure y and t_r discrimination. b) Optimal Q vs. t_r vs. energy with 90% confidence (crosses). Horizontal bars depict the energy range of calculation. Inset: Q vs t_r for 50-70 keV with 90% confidence (dotted), and $\frac{\beta}{\alpha}$ vs. t_r (faint line).

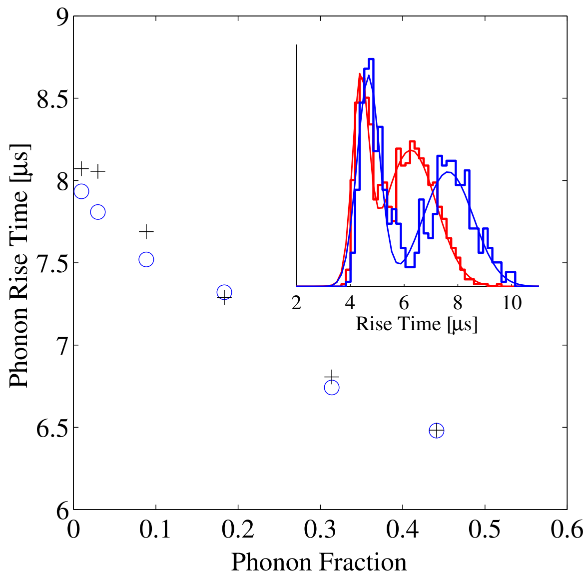

FIG. 3. A plot of phonon rise time for 60 keV photons vs. the fraction of phonon signal produced by drifting e-h pairs (circles); The model prediction (crosses). Inset: Rise time distributions for 0.1 volts and 3 volts (10% and 44%) with gaussian fits (solid line).